Memoirs of the School of Engineering, Okayama University, Vol. 19, No. 1, November 1984

Pore Water Pressure in Sand Bed under Oscillating Water Pressure

Hiroshi NAGŌ* and Shirō MAENO*

(Received September 29, 1984)

SYNOPSIS

In this paper the theoretical method to analyse the pore water pressures in the sand bed under the oscillating water pressure is developed. In the former researchs the validity of the theoretical treatment for the one-dimensional problem has been verified. However, the one-dimensional treatment is not sufficient to obtain the precise informations concerning the many practical problems. From this point of view, in this study, we derive the fundamental equations for the general three-dimensional sand layer under the oscillating water pressure. The validity of this theoretical method is verified by experiments for the two-dimensional problems.

1. INTRODUCTION

The authors have investigated the hydraulic behaviours of the pore water pressure and the effective stress in the sand bed under the oscillating water pressure as the basic research for the study on the dynamic behaviours of the sand bed itself and of the structures on the bed.

In the former researchs [1, 2] , in which the vertically one-dimensional sand layer was chosen as the subject of the study, the fundamental behaviours of the pore water pressures and the stresses in the

* Department of Civil Engineering

sand bed are clarified in relation to the properties of the oscillating water pressures and of the constituent materials. However, in the practical cases where several types of structures exist in or on the sand bed, the results obtained by the one-dimensional model are not sufficient to explain the behaviours around the structures. Two- or three-dimensional treatment becomes necessary in these cases.

In this study, from the above view point, we first derive the fundamental equations for the three-dimensional case. Then the pore water pressure distribution around the two-dimensional structures are analysed numerically by using these equations. Finally the theoretical results are verified by some experiments.

2. DERIVATION OF FUNDAMENTAL EQUATIONS

In the theoretical treatment of the present problem the following fundamental assumptions are adopted.

1) The sand and the water are compressible
2) The pore water moves in accordance with Darcy's law
3) The skeleton of the sand layer deforms in accordance with Hooke's law
4) The sand layer is composed of three phases; sand, water and air. Then, the porosity λ is the sum of the part for the water λ_w and the part for the air λ_a. That is,

$$\lambda = \lambda_w + \lambda_a \qquad \cdots(1)$$

Using these assumptions the fundamental equations are derived as follows.

Continuum equations for each phase are expressed as follows.

$$\partial[(1-\lambda)\rho_s]/\partial t + \nabla\cdot[\rho_s(1-\lambda)V_s] = 0 \quad \text{(for sand)} \qquad \cdots(2)$$

$$\partial(\lambda_w\rho_w)/\partial t + \nabla\cdot(\rho_w\lambda_w V_w) = 0 \quad \text{(for water)} \qquad \cdots(3)$$

$$\partial(\lambda_a\rho_a)/\partial t + \nabla\cdot(\rho_a\lambda_a V_a) = 0 \quad \text{(for air)} \qquad \cdots(4)$$

where, ∇ : vector operation,
t : time,
ρ_s : density of the sand grain,
ρ_w : density of the pore water,
ρ_a : density of the air,
V_s : velocity vector of the sand grain,

V_w : velocity vector of the pore water,

V_a : velocity vector of the air.

The equations of the state for each phase which constitutes the sand layer are assumed as follows.

$$\rho_s = \text{constant} \quad \cdots(5)$$

$$\rho_w = \rho_{w0}\exp(\beta p) \quad \cdots(6)$$

$$\rho_a = \rho_{a0}(P/P_0) \quad \cdots(7)$$

where, ρ_{w0}, ρ_{a0} : densities of the water and of the air under the atmospheric pressure,

β : compressibility of the water,

P : absolute pressure,

P_0 : atmospheric pressure,

p : pore water pressure.

Eq.(5) shows that the individual sand grains are imcompressible, Eq.(6) shows that the water is compressible with compressibility β, and Eq.(7) shows that compressibility of the air is in accordance with Boyle's law. Using the relationship, $P=P_0+p$, the changes of the densities with time and space are written as follows.

$$\partial\rho_s/\partial t = 0 \quad , \quad \nabla\rho_s = 0 \quad \cdots(8)$$

$$\partial\rho_w/\partial t = (\beta\rho_w)\partial p/\partial t \quad , \quad \nabla\rho_w = \beta\rho_w\nabla p \quad \cdots(9)$$

$$\partial\rho_a/\partial t = (\rho_a/P)\partial p/\partial t \quad , \quad \nabla\rho_a = (\rho_a/P)\nabla p \quad \cdots(10)$$

In the highly saturated sand layer,

$$1 - (\lambda_w/\lambda) \ll 1 .$$

Then, the relative velocity of the air to the pore water can be considered to be negligible, that is,

$$V_w = V_a$$

Substituting Eqs.(8), (9) and (10) into Eqs.(2), (3) and (4), we obtain the following equations.

$$\frac{\partial\lambda}{\partial t} + V_s\cdot\nabla\lambda - (1-\lambda)\nabla\cdot V_s = 0 \quad ...(11)$$

$$\frac{1}{\lambda_w}\frac{\partial\lambda_w}{\partial t} + \beta\frac{\partial p}{\partial t} + \frac{V_w\cdot\nabla(\rho_w\lambda_w)}{\rho_w\lambda_w} + \nabla\cdot V_w = 0 \quad ...(12)$$

$$\frac{1}{\lambda_a}\frac{\partial \lambda_a}{\partial t} + \frac{\rho_a}{P}\frac{\partial p}{\partial t} + \frac{V_w \cdot \nabla(\rho_a \lambda_a)}{\rho_a \lambda_a} + \nabla \cdot V_w = 0 \qquad \cdots(13)$$

Using Eq.(1) and the state Eqs.(9) and (10), we obtain the next equation from Eqs.(12) and (13).

$$\frac{1}{\lambda}\frac{\partial \lambda}{\partial t} + \frac{P\beta\lambda_w + \lambda_a}{P\lambda}\frac{\partial P}{\partial t} + V_w \cdot \left(\frac{1}{\lambda}\nabla\lambda + \frac{P\beta\lambda_w + \lambda_a}{P\lambda}\nabla P\right) + \nabla \cdot V_w = 0 \qquad \cdots(14)$$

Assuming that the water in the sand layer moves in accordance with Darcy's law,

$$q = \lambda_w(V_w - V_s) = -k\nabla\varphi \qquad \cdots(15)$$

where, φ : piezometric head,

$$\varphi = \int_{z_0}^{z} d\zeta + \frac{1}{g}\int_{P_0}^{P}\frac{d\xi}{\rho_w(\xi)} \qquad \cdots(16)$$

k : permeability coefficient,
P : pressure,
z : height (positive in upward direction),
P_0, z_0 : arbitrary reference values,
g : acceleration due to gravity.

From Eq.(15),

$$\nabla \cdot q = (V_w - V_s)\cdot\nabla\lambda_w + \lambda_w(\nabla\cdot V_w - \nabla\cdot V_s) = -k\nabla^2\varphi \qquad \cdots(17)$$

The term $\nabla^2\varphi$ in Eq.(17) is written as follows by using Eqs.(9) and (16)

$$\nabla^2\varphi = \frac{1}{\rho_w g}(\nabla^2 p - \beta\nabla p\cdot\nabla p) \qquad \cdots(18)$$

The elimination of the terms $\nabla\cdot V_w$ from Eqs.(14), (17) and (18) gives,

$$\left(\frac{k}{\rho_w g}\right)\nabla^2 P = V_w\left\{-\lambda\nabla\left(\frac{\lambda_w}{\lambda}\right) + \frac{\lambda_w}{P\lambda}(P\beta\lambda_w + \lambda_a)\nabla p\right\} + V_s\cdot\nabla\lambda_w + \lambda_w\nabla\cdot V_s$$
$$+ \frac{\lambda_w}{\lambda}\frac{\partial\lambda}{\partial t} + \frac{\lambda_w}{P\lambda}(P\beta\lambda_w + \lambda_a)\frac{\partial p}{\partial t} + \left(\frac{k}{\rho_w g}\right)\beta\nabla p\cdot\nabla p \qquad \cdots(19)$$

Eliminating the terms $\partial\lambda/\partial t$ from Eqs.(11) and (19),

$$\left(\frac{k}{\rho_w g}\right)\nabla^2 p = \frac{\lambda_w}{\lambda}\nabla\cdot V_s + \frac{\lambda_w}{P\lambda}(P\beta\lambda_w + \lambda_a)\frac{\partial p}{\partial t} + \lambda V_s\cdot\nabla\left(\frac{\lambda_w}{\lambda}\right)$$

$$+ \lambda V_w\cdot\left\{-\nabla\left(\frac{\lambda_w}{\lambda}\right) + \frac{\lambda_w}{P\lambda}(P\beta\lambda_w + \lambda_a)\nabla p\right\} + \left(\frac{k}{\rho_w g}\right)\beta\nabla p\cdot\nabla p \qquad ...(20)$$

Considering $\lambda_w/\lambda \fallingdotseq 1$ and neglecting the higher order terms, the following equation is obtained.

$$\left(\frac{k}{\rho_w g}\right)\nabla^2 p = \nabla\cdot V_s + \left(\beta\lambda_w + \frac{\lambda_a}{P}\right)\frac{\partial p}{\partial t} \qquad ...(21)$$

The above equation shows the relation between the pore water pressure p and the displacement velocity of the sand V_s. V_s is related to the displacement vector of the sand u_s as follows.

$$V_s = \partial u_s/\partial t \qquad ...(22)$$

The relation between the volumetric strain e and the displacement vector u_s is,

$$e = \nabla\cdot u_s \qquad ...(23)$$

Considering Eqs.(22) and (23), Eq.(21) can be rewritten as follows.

$$\left(\frac{k}{\rho_w g}\right)\nabla^2 p = \frac{\partial e}{\partial t} + \left(\beta\lambda_w + \frac{\lambda_a}{P}\right)\frac{\partial p}{\partial t} \qquad ...(24)$$

Eq.(24) contains two unknown quantities which are the pore water pressure p and the volumetric strain e. So, another one equation with respect to the displacement of the sand is necessary to obtain the pore water pressure. This equation has to be derived from the elastic behaviour of the sand.

Now we consider an elementary parallelepiped as shown in Fig.1. The components of the total stresses are denoted by τ^*_{xx}, τ^*_{yy}, τ^*_{zz} (nomal stresses) and τ^*_{xy}, τ^*_{yz}, τ^*_{zx} (shear stresses). If the effects of inertia forces are negligible small, the conditions of equilibrium can be written as follows.

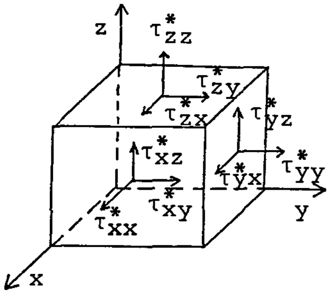

Fig.1 Elementary parallelepiped with total stresses

$$\frac{\partial \tau^*_{xx}}{\partial x} + \frac{\partial \tau^*_{xy}}{\partial y} + \frac{\partial \tau^*_{zx}}{\partial z} + F_x = 0$$

$$\frac{\partial \tau^*_{xy}}{\partial x} + \frac{\partial \tau^*_{yy}}{\partial y} + \frac{\partial \tau^*_{yz}}{\partial z} + F_y = 0 \qquad \text{...(25)}$$

$$\frac{\partial \tau^*_{zx}}{\partial x} + \frac{\partial \tau^*_{yz}}{\partial y} + \frac{\partial \tau^*_{zz}}{\partial z} + F_z = 0$$

where, F_x, F_y and F_z are the components of the body force per unit volume. The terms of nomal stresses τ^*_{xx}, τ^*_{yy} and τ^*_{zz} can be written in terms of effective stresses σ^*_x, σ^*_y, σ^*_z and of the pore water pressure p^*.

$$\tau^*_{xx} = \sigma^*_x - p^*$$

$$\tau^*_{yy} = \sigma^*_y - p^* \qquad \text{...(26)}$$

$$\tau^*_{zz} = \sigma^*_z - p^*$$

Each component of the stresses and the pore water pressure can be described by the sum of the initial state value and the incremental state value, for example $\sigma^*_x = \sigma^0_x + \sigma_x$ (σ^0_x denotes the initial stress, σ_x denotes the incremental stress). As for the body force in Eq.(25), it is independent of time because it is only gravitational one. Then, using the incremental components, Eq.(25) becomes,

$$\frac{\partial \sigma_x}{\partial x} + \frac{\partial \tau_{xy}}{\partial y} + \frac{\partial \tau_{zx}}{\partial z} = \frac{\partial p}{\partial x}$$

$$\frac{\partial \tau_{xy}}{\partial x} + \frac{\partial \sigma_y}{\partial y} + \frac{\partial \tau_{yz}}{\partial z} = \frac{\partial p}{\partial y} \qquad \text{...(27)}$$

$$\frac{\partial \tau_{zx}}{\partial x} + \frac{\partial \tau_{yz}}{\partial y} + \frac{\partial \sigma_z}{\partial z} = \frac{\partial p}{\partial y}$$

The above equilibrium equation is composed of the incremental stresses and pore water pressure. It is assumed that the stresses and strains of the sand layer are related each other by Hooke´s law in the following form.

$$\sigma_x = 2G\varepsilon_x + \lambda' e \quad , \quad \tau_{xy} = G\gamma_{xy}$$

$$\sigma_y = 2G\varepsilon_y + \lambda' e \quad , \quad \tau_{yz} = G\gamma_{yz} \qquad \text{...(28)}$$

$$\sigma_z = 2G\varepsilon_z + \lambda' e \quad , \quad \tau_{zx} = G\gamma_{zx}$$

where, ε_x , ε_y , ε_z : principal strains,
e : volumetric strain,
γ_x , γ_y , γ_z : shear strains,
G : shear modulus,
λ' : Lame's constant.

G and λ' are represented in the following forms by using Young's modulus and Poisson's ratio.

$$G = E/2(1 + \nu)$$

$$\lambda' = \nu/(1 + \nu)(1 - 2\nu)E$$

In the case of small deformation, the strains are related to the displacement components as follows.

$$\varepsilon_x = \partial u_x/\partial x \quad , \quad \gamma_{xy} = \partial u_x/\partial y + \partial u_y/\partial x$$
$$\varepsilon_y = \partial u_y/\partial y \quad , \quad \gamma_{yz} = \partial u_y/\partial z + \partial u_z/\partial y \qquad \ldots(29)$$
$$\varepsilon_z = \partial u_z/\partial z \quad , \quad \gamma_{zx} = \partial u_z/\partial x + \partial u_x/\partial z$$

Substituting Eqs.(28) and (29) into Eq.(27), following equations are obtained.

$$G\nabla^2 u_x + [G/(1-2\nu)](\partial e/\partial x) = \partial p/\partial x$$
$$G\nabla^2 u_y + [G/(1-2\nu)](\partial e/\partial y) = \partial p/\partial y \qquad \ldots(30)$$
$$G\nabla^2 u_y + [G/(1-2\nu)](\partial e/\partial z) = \partial p/\partial z$$

Consequently the distributions of the pore water pressure and the stresses in the three-dimensional sand layer are obtained by solving Eqs.(24) and (30). In the practical problems appeared in the river and coastal engineering, there are many structures considered to be vertically two-dimensional. For such cases Eqs.(24) and (30) are reduced as follows.

$$G\left(\frac{\partial^2 u_x}{\partial x^2} + \frac{\partial^2 u_x}{\partial z^2}\right) + \frac{G}{1-2\nu}\frac{\partial}{\partial x}\left(\frac{\partial u_x}{\partial x} + \frac{\partial u_z}{\partial z}\right) = \frac{\partial p}{\partial x}$$
$$G\left(\frac{\partial^2 u_z}{\partial x^2} + \frac{\partial^2 u_z}{\partial z^2}\right) + \frac{G}{1-2\nu}\frac{\partial}{\partial z}\left(\frac{\partial u_x}{\partial x} + \frac{\partial u_z}{\partial z}\right) = \frac{\partial p}{\partial z} \qquad \ldots(31)$$
$$\left(\beta\lambda_w + \frac{\lambda_a}{P}\right)\frac{\partial p}{\partial t} + \frac{\partial}{\partial t}\left(\frac{\partial u_x}{\partial x} + \frac{\partial u_z}{\partial z}\right) = \frac{k}{\rho_w g}\left(\frac{\partial^2 p}{\partial x^2} + \frac{\partial^2 p}{\partial z^2}\right)$$

Generally, the partial differential equations obtained above are analysed numerically by using the finite difference method or finite element method or the like. Considering the merits of the finite element method which are applicable to any boundary conditions and any bed materials, here, we adopt the finite element method to solve the equations. Next, the governing equations for two-dimensional problem are transformed into finite element equations as follows.

3. FINITE ELEMENT FORMULATION

The Galerkin method which is one of the weighted residual method is used to obtain a numerical solution of the system of Eq.(31). Now we put Eq.(31) into the following equations.

$$L_1(u_x,u_z,p) = G\left(\frac{\partial^2 u_x}{\partial x^2}+\frac{\partial^2 u_x}{\partial z^2}\right)+\frac{G}{1-2\nu}\frac{\partial}{\partial x}\left(\frac{\partial u_x}{\partial x}+\frac{\partial u_z}{\partial z}\right)-\frac{\partial p}{\partial x}=0 \quad \ldots(32\text{-a})$$

$$L_2(u_x,u_z,p) = G\left(\frac{\partial^2 u_z}{\partial x^2}+\frac{\partial^2 u_z}{\partial z^2}\right)+\frac{G}{1-2\nu}\frac{\partial}{\partial z}\left(\frac{\partial u_x}{\partial x}+\frac{\partial u_z}{\partial z}\right)-\frac{\partial p}{\partial z}=0 \quad \ldots(32\text{-b})$$

$$L_3(u_x,u_z,p) = \left(\beta\lambda_w+\frac{\lambda}{P}\right)\frac{\partial p}{\partial t}+\frac{\partial}{\partial t}\left(\frac{\partial u_x}{\partial x}+\frac{\partial u_z}{\partial z}\right)-\frac{k}{\rho_w g}\left(\frac{\partial^2 p}{\partial x^2}+\frac{\partial^2 p}{\partial z^2}\right)=0 \quad (32\text{-c})$$

In the finite element method the continuous functions u_x, u_z and p are replaced by the values of the function specified at a finite number of nodes. Therefore, the analytical region is devided in to a finite number of elements. Using the functions of time and space correspond to a finite number of nodes, the pore water pressures and the displacements in the elements are represented as follows.

$$u_x(x,z,t) = \sum_{j=1}^{N} a_j(t)\cdot\phi_j^x(x,z) \quad \ldots(33\text{-a})$$

$$u_y(x,z,t) = \sum_{j=1}^{N} b_j(t)\cdot\phi_j^y(x,z) \quad \ldots(33\text{-b})$$

$$p\,(x,z,t) = \sum_{j=1}^{N} c_j(t)\cdot\phi_j^p(x,z) \quad \ldots(33\text{-c})$$

where, a_j, b_j and c_j are the nodal values of u_x, u_y and p respectively. They are the functions dependent only on time. While, ϕ_j^x, ϕ_j^z, ϕ_j^p are the shape functions dependent only on coordinates. Applying the

Galerkin method to Eq.(32),

$$\int L_1(u_x,u_z,p)\,\phi_i^x ds = 0 \quad , \quad i = 1,2,\cdots,N \qquad \cdots(34\text{-a})$$

$$\int L_2(u_x,u_z,p)\,\phi_i^y ds = 0 \quad , \quad i = 1,2,\cdots,N \qquad \cdots(34\text{-b})$$

$$\int L_3(u_x,u_z,p)\,\phi_i^p ds = 0 \quad , \quad i = 1,2,\cdots,N \qquad \cdots(34\text{-c})$$

Using the relationship of Eq.(33) after substituting Eq.(32) into Eq.(34), and applying Green's theorem to the terms involving second derivatives with respect to x and z,

$$\sum_{j=1}^{N}\Big[\Big\{(\lambda'+2G)\int \frac{\partial\phi_j^x}{\partial x}\frac{\partial\phi_i^x}{\partial x}ds + G\int \frac{\partial\phi_j^x}{\partial z}\frac{\partial\phi_i^x}{\partial z}ds\Big\}a_j + \Big\{(\lambda'+G)\int\frac{\partial\phi_j^z}{\partial z}\frac{\partial\phi_i^x}{\partial x}ds\Big\}b_j + \Big(\int \frac{\partial\phi_j^p}{\partial x}\phi_i^x ds\Big)c_j\Big] = (\lambda'+2G)\int n_x \frac{\partial u_x}{\partial x}\phi_i^x d\ell$$

$$+ G\int n_z \frac{\partial u_x}{\partial z}\phi_i^x d\ell + (\lambda'+G)\int n_x\frac{\partial u_z}{\partial z}\phi_i^x d\ell \qquad \cdots(35\text{-a})$$

$$\sum_{j=1}^{N}\Big[\Big\{(\lambda'+G)\int \frac{\partial\phi_j^x}{\partial x}\frac{\partial\phi_i^z}{\partial z}ds\Big\}a_j + \Big\{(G\int \frac{\partial\phi_j^z}{\partial x}\frac{\partial\phi_i^z}{\partial x}ds + (\lambda'+2G)\int \frac{\partial\phi_j^z}{\partial z}\frac{\partial\phi_i^z}{\partial z}ds\Big\}b_j$$

$$+ \Big(\int \frac{\partial\phi_j^p}{\partial z}\phi_i^z ds\Big)c_j\Big] = G\int n_x \frac{\partial u_z}{\partial x}\phi_i^z d\ell$$

$$+ (\lambda'+2G)\int n_z \frac{\partial u_z}{\partial z}\phi_i^z d\ell + (\lambda'+G)\int n_z \frac{\partial u_x}{\partial x}\phi_i^z d\ell \qquad \cdots(35\text{-b})$$

$$\sum_{j=1}^{N}\Big[\Big(\int \frac{\partial\phi_j^x}{\partial x}\phi_i^p ds\Big)\frac{\partial a_j}{\partial t} + \Big(\int \frac{\partial\phi_j^z}{\partial z}\phi_i^p ds\Big)\frac{\partial b_j}{\partial t} + \Big\{(\beta\lambda_w + \frac{\lambda_a}{P})\int \phi_j^p\phi_i^p ds\Big\}\frac{\partial c_j}{\partial t}$$

$$+ \frac{k}{\rho_w g}\Big(\int \frac{\partial\phi_j^p}{\partial x}\frac{\partial\phi_i^p}{\partial x}ds + \int \frac{\partial\phi_j^p}{\partial z}\frac{\partial\phi_i^p}{\partial z}ds\Big)c_j\Big]$$

$$= \frac{k}{\rho_w g}\Big(\int n_x \frac{\partial p}{\partial x}\phi_i^p d\ell + \int n_z \frac{\partial p}{\partial z}\phi_i^p d\ell\Big) \qquad \cdots(35\text{-c})$$

where, n_x, n_z : direction cosines in x- and z-direction respectively,
ℓ : integration along the boundary.

For the terms with respect to time a finite difference method is applied. In general the finite difference formulation is as follows.

$$\partial f_j/\partial t = (f_j^{t+\Delta t} - f_j^{t})/\Delta t \quad , \quad f_j = \theta f_j^{t+\Delta t} + (1-\theta) f_j^{t}$$

where, $\theta=0$ represents an explicit forward difference scheme, $\theta=1/2$ represents a centered difference scheme (Crank Nicholson scheme) and $\theta=1$ represents a fully implicit backward difference scheme in time. Using above relationships and introducing the matrix notation, Eq.(35) becomes as follows.

$$\begin{bmatrix} \theta A_{ij} & \theta B_{ij} & \theta C_{ij} \\ \theta D_{ij} & \theta E_{ij} & \theta F_{ij} \\ \frac{1}{\Delta t}H_{ij} & \frac{1}{\Delta t}P_{ij} & \frac{\beta\lambda_w+\lambda_a/P}{\Delta t}Q_{ij}+\frac{\theta k}{\rho_w g}R_{ij} \end{bmatrix}^{t+\Delta t} \begin{Bmatrix} a_j \\ b_j \\ c_j \end{Bmatrix}$$

$$= \begin{bmatrix} (\theta-1)A_{ij} & (\theta-1)B_{ij} & (\theta-1)C_{ij} \\ (\theta-1)D_{ij} & (\theta-1)E_{ij} & (\theta-1)F_{ij} \\ \frac{1}{\Delta t}H_{ij} & \frac{1}{\Delta t}P_{ij} & \frac{\beta\lambda_w+\lambda_a/P}{\Delta t}Q_{ij}+\frac{(\theta-1)k}{\rho_w g}R_{ij} \end{bmatrix}^{t} \begin{Bmatrix} a_j \\ b_j \\ c_j \end{Bmatrix} + \begin{Bmatrix} F_i^{(1)} \\ F_i^{(2)} \\ F_i^{(3)} \end{Bmatrix} \quad (36)$$

where,

$$A_{ij}=(\lambda'+2G)\int\frac{\partial\phi_j^x}{\partial x}\frac{\partial\phi_i^x}{\partial x}ds+G\int\frac{\partial\phi_j^x}{\partial z}\frac{\partial\phi_i^x}{\partial z}ds \quad \cdots(36\text{-a})$$

$$B_{ij}=(\lambda'+G)\int\frac{\partial\phi_j^z}{\partial z}\frac{\partial\phi_i^x}{\partial x}ds \quad \cdots(36\text{-b})$$

$$C_{ij}=\int\frac{\partial\phi_j^p}{\partial x}\phi_i^x ds \quad \cdots(36\text{-c})$$

$$D_{ij}=(\lambda'+G)\int\frac{\partial\phi_j^x}{\partial x}\frac{\partial\phi_i^z}{\partial z}ds \quad \cdots(36\text{-d})$$

$$E_{ij}=G\int\frac{\partial\phi_j^z}{\partial x}\frac{\partial\phi_i^z}{\partial x}ds+(\lambda'+2G)\int\frac{\partial\phi_j^z}{\partial z}\frac{\partial\phi_i^z}{\partial z}ds \quad \cdots(36\text{-e})$$

$$F_{ij}=\int\frac{\partial\phi_j^p}{\partial z}\phi_i^z ds \quad \cdots(36\text{-f})$$

$$H_{ij}=\int\frac{\partial\phi_j^x}{\partial x}\phi_i^p ds \quad \cdots(36\text{-g})$$

$$P_{ij}=\int\frac{\partial\phi_j^z}{\partial z}\phi_i^p ds \quad \cdots(36\text{-h})$$

$$Q_{ij}=\int\phi_j^p\phi_i^p ds \quad \cdots(36\text{-i})$$

$$R_{ij}=\int\frac{\partial\phi_j^p}{\partial x}\frac{\partial\phi_i^p}{\partial x}ds+\int\frac{\partial\phi_j^p}{\partial z}\frac{\partial\phi_i^p}{\partial z}ds \quad \cdots(36\text{-j})$$

$$\{F_i^{(1)}\}=(\lambda'+2G)\int n_x\frac{\partial ux}{\partial x}\phi_i^x d\ell+G\int n_z\frac{\partial ux}{\partial z}\phi_i^x d\ell+(\lambda'+G)\int n_z\frac{\partial uz}{\partial z}\phi_i^x d\ell \quad \cdots(36\text{-k})$$

$$\{F_i^{(2)}\}=G\int n_x\frac{\partial uz}{\partial x}\phi_i^z d\ell+(\lambda'+2G)\int n_z\frac{\partial uz}{\partial z}\phi_i^z d\ell+(\lambda'+G)\int n_z\frac{\partial ux}{\partial x}\phi_i^z d\ell \quad \cdots(36\text{-l})$$

$$\{F_i^{(3)}\}=\frac{k}{\rho_w g}\left(\int n_x\frac{\partial p}{\partial x}\phi_i^p d\ell+\int n_z\frac{\partial p}{\partial z}\phi_i^p d\ell\right) \quad \cdots(36\text{-m})$$

where, repeated indices i,j=1,2, ··· N indicates the summation. The above equations are solved every incremental small time step after the formation of linear system of equations.

4. OUTLINE OF NUMERICAL ANALYSIS OF VERTICAL TWO-DIMENSIONAL SAND LAYER MODEL

4.1 Models for the Analysis

For the analysis the vertical two-dimensional sand layer models as shown in Fig.2 are treated. Models are the sand layers around the structure hatched in the figure. The thickness of the structure is d. The thickness of the layer is D. In one of the models the sheet pile with the length ℓ shown by dashed line is set up in front nose of the structure. They are considered to be simplified models of many

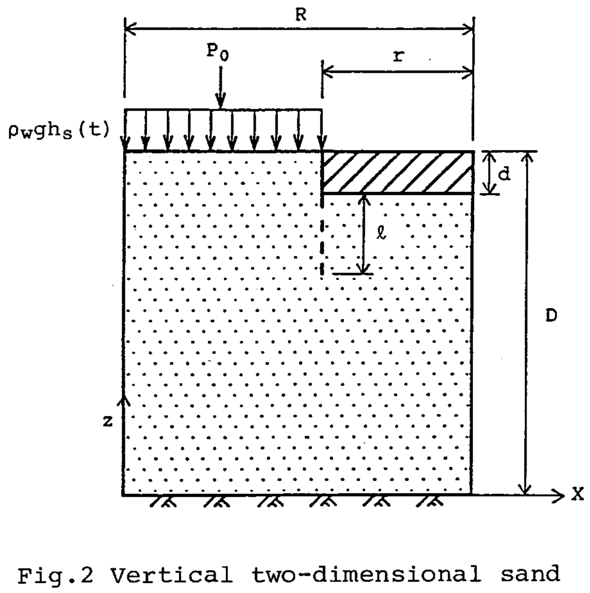

Fig.2 Vertical two-dimensional sand layer model in analysis

typical hydraulic structures. The oscillating water pressure $\rho_w g h_s(t)$ acts on the surface of the sand bed in front of the structure.

4.2 Fundamental Equations and Boundary Conditions

For the above mentioned models, putting $P=P_0+\rho_w gh$ and $p=\rho_w gh$, Eq.(31) becomes as follows.

$$G\left(\frac{\partial^2 u_x}{\partial x^2}+\frac{\partial^2 u_x}{\partial z^2}\right)+\frac{G}{1-2\nu}\frac{\partial}{\partial x}\left(\frac{\partial u_x}{\partial x}+\frac{\partial u_z}{\partial z}\right)=\rho_w g\frac{\partial h}{\partial x}$$

$$G\left(\frac{\partial^2 u_z}{\partial x^2}+\frac{\partial^2 u_z}{\partial z^2}\right)+\frac{G}{1-2\nu}\frac{\partial}{\partial z}\left(\frac{\partial u_x}{\partial x}+\frac{\partial u_z}{\partial z}\right)=\rho_w g\frac{\partial h}{\partial z} \qquad (37)$$

$$\rho_w g\left(\beta\lambda_w+\frac{\lambda a}{P_0+\rho_w gh}\right)\frac{\partial h}{\partial t}+\frac{\partial}{\partial t}\left(\frac{\partial u_x}{\partial x}+\frac{\partial u_z}{\partial z}\right)=k\left(\frac{\partial^2 h}{\partial x^2}+\frac{\partial^2 h}{\partial z^2}\right)$$

where, h : head of pore water pressure.

Eq.(37) are analysed under the following boundary conditions.

For the case without sheet pile,

$h=h_s(t)$ at $(0\leqq x\leqq R-r\ ,\ z=D)$

$\partial h/\partial z=0\ ,\ u_z=0$ at $(0\leqq x\leqq R\ ,\ z=0)$ and $(R-r\leqq x\leqq R\ ,\ z=D-d)$

$\partial h/\partial x=0\ ,\ u_x=0$ at $(x=0\ ,\ 0\leqq z\leqq D)\ ,\ (x=R\ ,\ 0\leqq z\leqq D-d)$ and $(x=R-r\ ,\ D-d\leqq z\leqq D)$

For the case with sheet pile, the following condition is added to the above conditions.

$\partial h/\partial x=0\ ,\ u_x=0$ at $(x=R-r\ ,\ D-d-\ell\leqq z\leqq D-d)$

4.3 Method and Conditions of Calculation

Numerical calculation was carried out by using the Gelerkin finite element method as is mentioned in chapter 2. One example of the finite element mesh is shown in Fig.3.

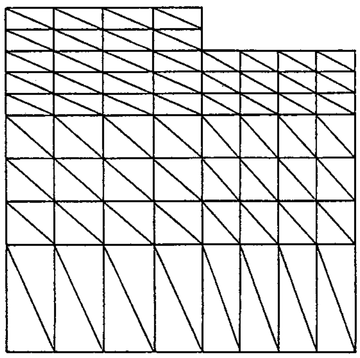

Fig.3 Finite element mesh

In the calculations as the oscillating water pressure h_s acting on the surface of the sand layer the values obtained by the experiment are used. Taking into account the experiment, the values of each constants in basic equations adopted to the calculation are as follows.

$\lambda_a = 0.003$, $\lambda_w = 0.4$, $k = 0.15$ cm/sec ,
$\beta = 43.8 \times 10^{-10}$ m^2/kg (44.6×10^{-11} m^2/N),
$G = 1.69 \times 10^6$ kg/m^2 (1.65×10^7 N/m^2),
$\nu = 0.48$.

5. EXPERIMENTS AND NUMERICAL ANALYSIS

5.1 Experimental Apparatus and Procedure

For the experiment the vertical two-dimensional model as shown in Fig.4 was used. The depth of the model is 40cm. It is filled with the highly saturated sand (Toyoura standard sand $d_{50} \fallingdotseq 0.25$mm). The water depth over the sand surface is about 110cm. The sinusoidally oscillating air pressure acts on the water surface. It's amplitude is about 40cm in water head. The frequency is about 0.9Hz. The experiment was carried out for four cases shown in Table 1. The depth of the structure is changed in the experiments for case 1 and case 2, where the sheet pile is not located. The length of the sheet pile is changed in the experiment for case 3 and case 4, where the depth of the structure remains the same.

Table 1 Experimental conditions

case	d(cm)	ℓ(cm)
1	10.0	0.0
2	30.0	0.0
3	10.0	20.0
4	10.0	30.0

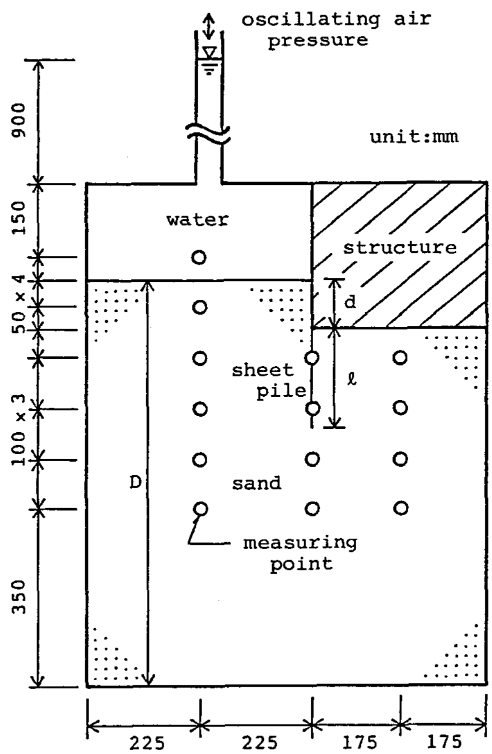

Fig.4 Experimental apparatus

5.2 Experimental and Theoretical Results

Fig.5 and Fig.6 show the experimental and theoretical results of the change of the time history of the pore water pressure in the vertical direction for case 1. Fig.7 and Fig.8 show the same ones in the horizontal direction for case 1 and case 2 respectively. In these figures h_0 is the head of mean water pressure h_s on the sand surface. From these figures it is shown that the theoretical results explain fairly well the behaviours of the pore water pressure obtained by the experiments. Around the structure placed in the sand layer the pore water pressures propagate with the damping in amplitude and with the lag in phase not only in the vertical direction but also in the horizontal direction. Especially under the structure, both the damping in amplitude and the lag in phase are considerably large.

Fig.9 shows the time history of the pore water pressure around the sheet pile (case 3). From this figure, the theoretical results explain fairly well the characteristics of the damping and the lag obtained by the experiment. Inside of the sheet pile, the damping in amplitude and the lag in phase are very large and the change of them in the vertical direction are small.

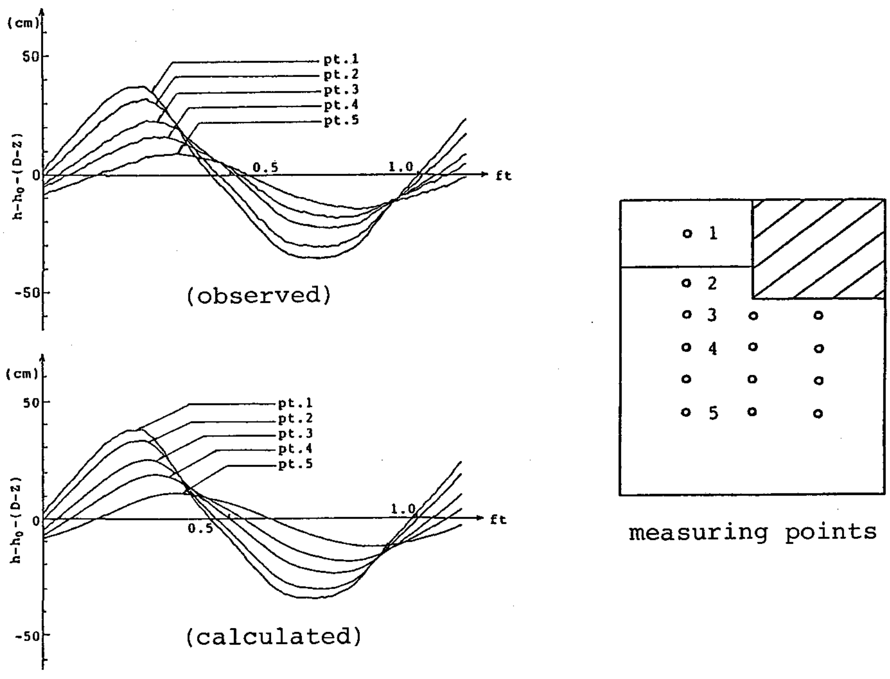

Fig.5 Pore water pressure(case 1, vertical distribution)

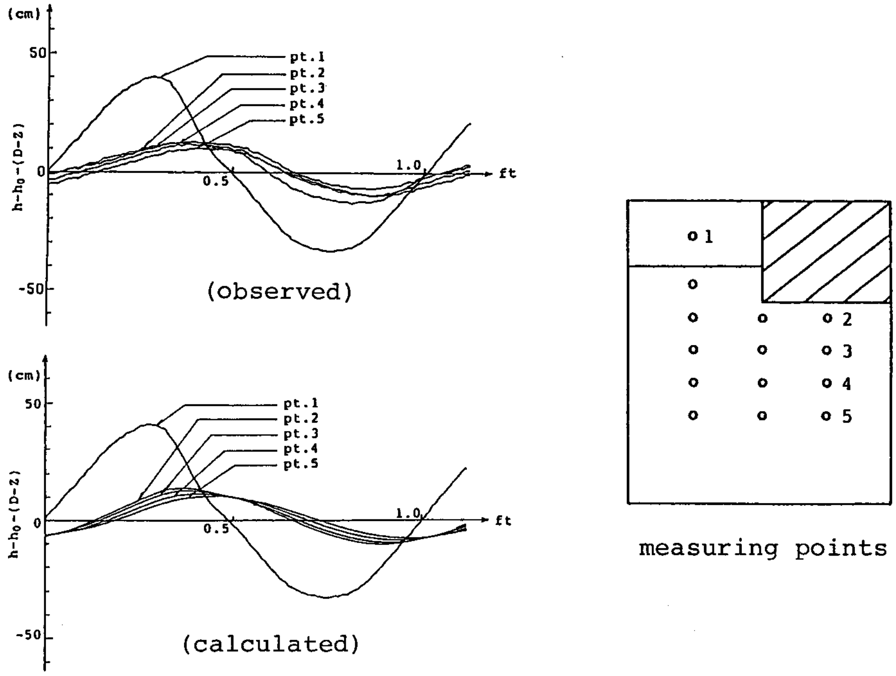

Fig.6 Pore water pressure(case 1, vertical distribution)

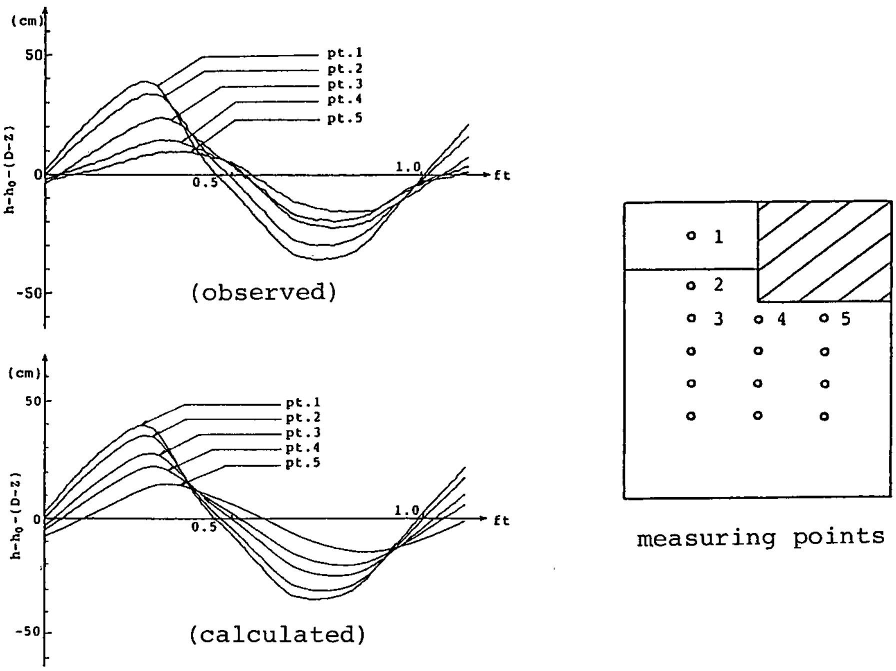

Fig.7 Pore water pressure(case 1, horizontal distribution)

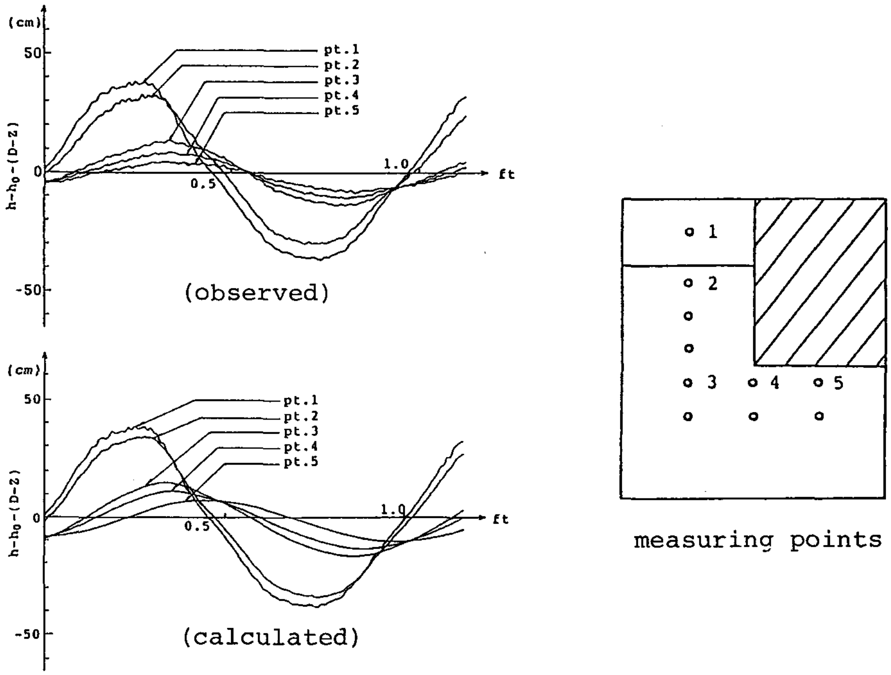

Fig.8 Pore water pressure(case 2, horizontal distribution)

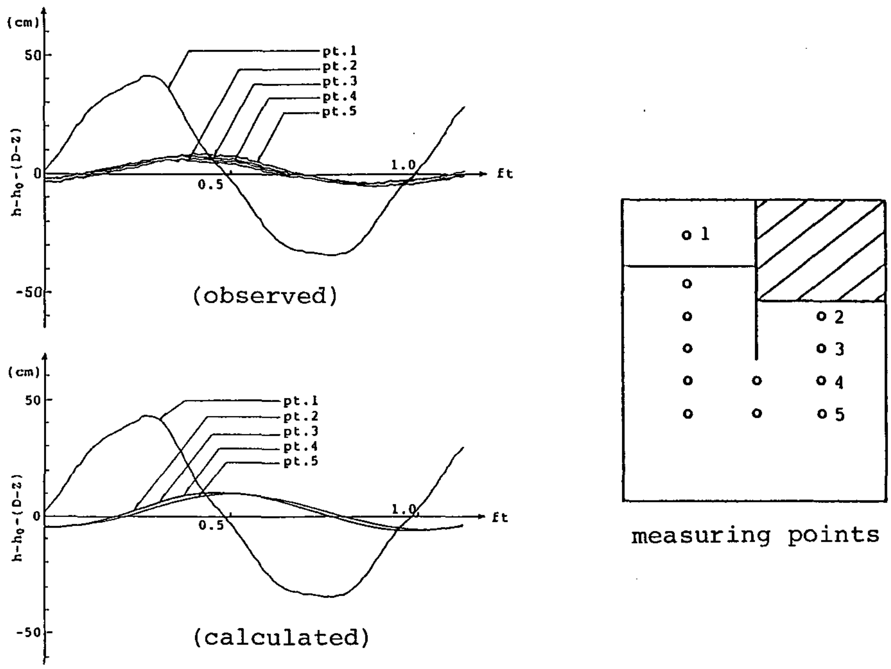

Fig.9 Pore water pressure(case 3, vertical distribution)

Fig.10 shows the damping in amplitude and the lag in phase under the structure for the cases with and without sheet pile. About the damping in amplitude, in the case without sheet pile the damping propagates from upper layer to lower layer, while in the case with sheet pile the damping propagates from lower layer to upper layer. That is, the propagation route of the pore water pressure changes by setting the sheet pile. About the lag in phase, similar phenomenon appears. Comparing experimental results with theoretical ones, in the case without sheet pile, both of them are in a good agreement in quantity, while in the case with sheet pile, the considerable difference is recognized in quantity, though the decreasing tendency is the same. Concerning this difference the room for examination remains in the finite element mesh near the point of sheet pile.

Fig.11 shows the state of liquefaction of sand around the structure. This phenomenon was obserbed only in the experiment for case 1. The blank part in the sand layer in Fig.11 shows the region where the sand moves. This phenomenon seems to be caused by the horizontal

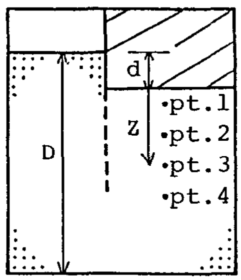

measuring points

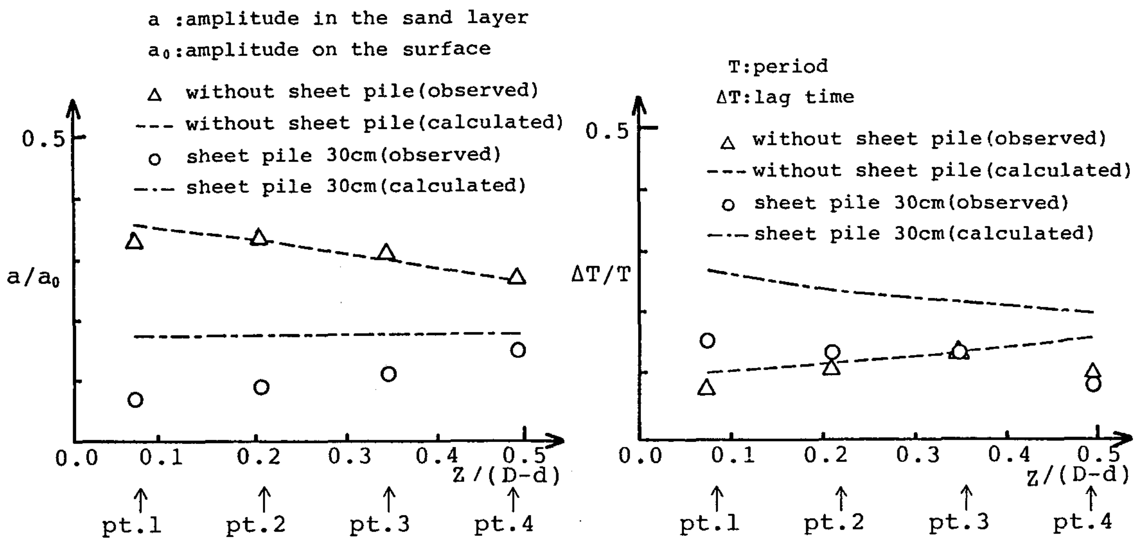

(1) Damping in amplitude (2) Lag in phase

Fig.10 Damping in amplitude and lag in phase under the structure difference of the pore water pressure which occurs under the structure as the results of the damping and the lag in the horizontal direction.

Fig.12 shows the horizontal distribution of the pore water pressure under the structure in the experiment for case 1. The point numbers in this figure are the same ones in the Fig.7. In this figure, the maximum difference of the pore water pressure h′ is about 5cm. This difference cause the horizontal seepage force. Fig.13 shows the same results for case 2. In this figure, the difference of the pore water pressure is in the same degree with ones for case 1. But

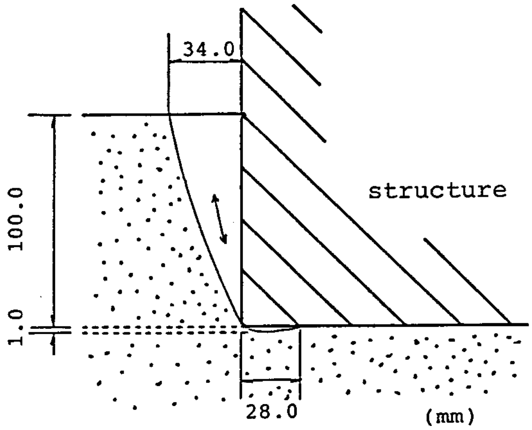

Fig.11 The state of liquefaction

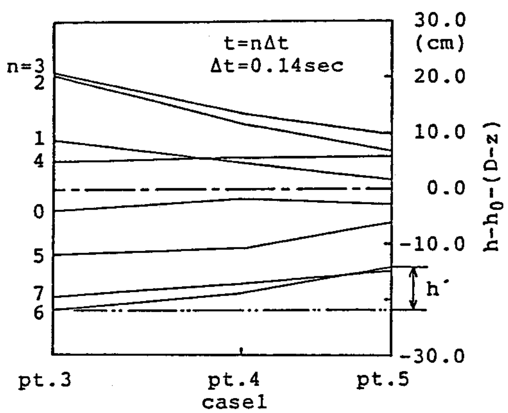

Fig.12 Horizontal distribution of the pore water pressure

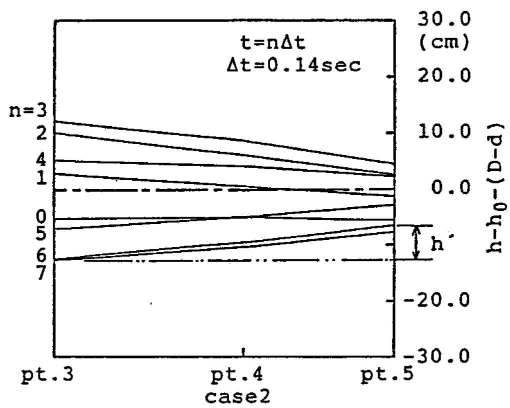

Fig.13 Horizontal distribution of the pore water pressure

the movement of the sand does not occur. In this case it is considered that the horizontal shearing registance force becomes larger than the seepage force. That is, the superimposed load becomes larger because the depth of the structure in case 3 is larger than that in case 1.

6. CONCLUDING REMARKS

In this paper the pore water pressure under the oscillating water pressure in the sand layer was treated theoretically and experimentally. Conclusions obtained through the research are as follows.

Experimental results on the pore water pressure are explained fairly well by the theoretical analysis. Then, it may be concluded that the method of this theoretical analysis give an appropriate solution of the pore water pressure in the two-dimensional sand layer.

In this paper we have tried the qualitative explanation of the relationship between the pore water pressure distribution around the structure and the dynamic behaviours of the sand layer. On the basis of this study, the subject for a future study is the establishment of the quantitative estimation method, and of the rational design method of the hydraulic structures in regard to the practical engineering problems, scouring, sinking, sucking out, etc.

ACKNOWLEDGEMENT

The authors wish to express their gratitude to Kinji Takai, Tōru Akune, Syōji Itō, Hironori Fnahashi and Kimiaki Satomoto for their asistances in experiments and computations.

REFERENCES

[1] H. Nago : Liquefaction of Highly Saturated Sand Layer under Oscillating Water Pressure, Memoirs of the School of Engineering, Okayama Univ., Vol.16, No.1, 1981, pp.91-104.

[2] S. Maeno and H. Nago : Effect of Displacement Method on Sand Bed Liquefaction under Oscillating Water Pressure, Memoirs of the School of Engineering, Okayama Univ., Vol.17, No.1, 1983, pp.61-71.

[3] Biot, M.A. : General Theory of Three-dimensional Consolidation, J. Appl. Phys. 12, 1941, pp. 155-164.

[4] De Wiest, R. J. M. : Flow through Porous Media, Acad. Press, New York and London, 1969, pp. 337-344.